

Stellar occultation predictions for 9 irregular satellites of giant planets and Triton for 2015-2017

A. R. Gomes-Júnior¹, M. Assafin^{1,*}, R. Vieira-Martins^{1,2,3,**}, J. I. B. Camargo^{2,3}, B. E. Morgado¹,

¹ Observatório do Valongo/UFRJ, Ladeira Pedro Antônio 43, CEP 20.080-090 Rio de Janeiro - RJ, Brazil
e-mail: altair08@astro.ufrj.br

² Observatório Nacional/MCT, R. General José Cristino 77, CEP 20921-400 Rio de Janeiro - RJ, Brazil
e-mail: rvm@on.br

³ Laboratório Interinstitucional de e-Astronomia - LIneA, Rua Gal. José Cristino 77, Rio de Janeiro, RJ 20921-400, Brazil

Received ; accepted

ABSTRACT

Key words. Occultations - Planets and satellites: general - Planets and satellites: individual: Jovian and Saturnian irregular satellites

1. Introduction

Irregular (outer) satellites revolve around giant planets at large distances in eccentric, highly inclined and frequently retrograde orbits. Because of these peculiar orbits, it is largely accepted that these objects were not originated with, but were captured by their planets in the early solar system (Sheppard 2005).

There is a number of capture mechanisms of objects by giant planets proposed in the literature. There is the Gas Drag in the primordial circumplanetary nebulae (Sheppard 2005) where the object would be affected by the gas drag and its velocity slowed down until it be captured by the planet. Another mechanism is called pull-down capture (Sheppard 2005), where the mass of the planet would increase while the object was temporarily captured.

A mechanism based in the Nice model (Morbidelli et al. 2005; Tsiganis et al. 2005; Gomes et al. 2005) was proposed by Nesvorný et al. (2007) and, in the specific case of Jupiter with the modern Nice model, by Nesvorný et al. 2014. During the early solar system instability, encounters between the outer planets occurred. These planetary encounters could exchange energy and angular momentum between planets and the objects nearby making it possible for the capture of irregular bodies by the giant planets. In this scenario, the survival rate of prior-LHB (Late Heavy Bombardment) satellites is very small.

Another important mechanism is the capture through collisional interactions (Sheppard 2005). A collision between two small bodies in the Hill's sphere of the planet could generate fragmented objects and the dissipated energy could be such that some of these objects could be captured.

Some of these objects are in dynamical groups with similar orbital elements, called families, similar to families found in the Main Asteroid Belt. These families may have been created by a parent body disrupted by collisions with comets or other satel-

lites (Nesvorný et al. 2004). Collisions with comets are more likely to have occurred during the LHB (Gomes et al. 2005).

Nesvorný et al. (2003) studied the collision rates between irregular satellites and concluded that some satellites could have been removed by collision with a bigger satellite. The collision rate between satellites of the Himalia Group (Himalia, Elara, Lysithea and Leda, mainly), for instance, was found to be more than one during the solar system age suggesting that their current structure was originated by satellite-satellite collision.

For Phoebe, ejected material from its surface caused by impacts could evolve due to Poynting-Robertson drag and collide with Iapetus causing the large variation in albedo observed on it (Nesvorný et al. 2003). Indeed, Cassini was able to detect in Phoebe an absorption feature at $2.42 \mu\text{m}$ (probably CN combinations) that was also detected in the dark side of Iapetus (Clark et al. 2005).

The region of origin of these object is not well known. Grav et al. (2003) and Grav & Bauer (2007) showed that the irregular satellites from the giant planets have their colors and spectral slopes similar to C-, D- and P-type asteroids, Centaurs and trans-neptunian objects (TNOs) suggesting that they have been originated from different locations in the early solar system.

In this work, we propose to study these objects as possible representatives of the small TNOs' population. The basis for this hypothesis is discussed in Section 2. TNOs are highly interesting objects that due to their large heliocentric distances (low temperatures) may be highly preserved having their physical properties similar to those they had when they were formed, then providing history and evolution of the outer solar system (Camargo et al. 2013). This is even more true for the smaller objects, since in principle larger sizes favour physical differentiation processes in the body and vice-versa. However, due to the distance, the smaller TNOs from this region are more difficult to observe. A clever way to overcome this difficulty is to study the much closer irregular satellites, under the hypothesis that they share a common origin with the small TNOs' population.

In order to obtain precise fundamental physical parameters like size, shape and albedo for the irregular satellites (and thus, in a sense, to small-sized TNOs), we will make use of stellar occul-

Send offprint requests to: A. R. Gomes-Júnior

* Affiliated researcher at Observatoire de Paris/IMCCE, 77 Avenue Denfert Rochereau 75014 Paris, France

** Affiliated researcher at Observatoire de Paris/IMCCE, 77 Avenue Denfert Rochereau 75014 Paris, France

Table 1. Estimated diameter of the satellites and correspondent apparent diameter

Satellite	Diameter of the satellites		References
	km	mas ^a	
Ananke	29		1
Carme	46		1
Elara	86		1
Himalia	$(150 \pm 20) \times (120 \pm 20)$		2
Lysithea	36		1
Pasiphae	62		1
Sinope	37		1
Phoebe	212 ± 1.4		3
Nereid	340 ± 50		4
Triton	2707 ± 2.0		5

References. (1) Rettig et al. (2001); (2) Porco et al. (2003); (3) Thomas (2010); (4) Thomas et al. (1991) (5) Thomas (2000).

^(a) Using a mean distance from Jupiter of XX AU, from Saturn of XX AU and from Neptune of XX AU.

tations, which provide more accurate results than other ground-based techniques (Sicardy et al. 2011; Ortiz et al. 2012; Braga-Ribas et al. 2014).

Up to date no stellar occultation by irregular satellite is found in the literature. Since their estimated sizes are very small (see table 1), prediction of the exact location and instant where the shadow will cross the Earth demands a good accurate ephemeris and star positions. For instance, Himalia, supposedly the largest irregular satellite of Jupiter has an estimated size of 150 km (Porco et al. 2003), which is equivalent to an apparent size of about 40 mas (milliarcseconds). Thus, even in the best cases, the overall budget of ephemeris and star position errors must be around 40 mas in order that we get good chances of observing a stellar occultation.

Unlikely stellar occultations by TNOs, which has been proved effective, the observation of an occultation by a irregular satellite is more favorable. They have been known for more time and observed in many orbital period having better ephemeris than TNOs. Moreover, the irregular satellites are closer to Earth which means a minor error in kilometers.

Gomes-Júnior et al. (2015) obtained 6523 suitable positions for 18 irregular satellites between 1992 and 2014 with an estimated error in the positions of about 60 to 80 mas. For some satellites the number of positions obtained is comparable to the number used in the numerical integration of orbits by the JPL (Jacobson et al. 2012). They pointed out that the ephemeris of the irregular satellites have systematic errors that may reach 200 mas for some satellites. For an object at the distance of Jupiter, this represents an error bigger than 700 km in the shadow path. Using the offsets obtained by Gomes-Júnior et al. (2015) it is possible to correct the ephemeris and better predict stellar occultations for these objects.

We present in this paper stellar occultation predictions for the 7 major irregular satellites of Jupiter (Himalia, Elara, Pasiphae, Lysithea, Carme, Ananke and Sinope), Phoebe from Saturn and Nereid from Neptune. In the section 2 we explore the scientific rationale for the study of the irregular satellites and the possibility of having a common origin with TNOs. In section 3 we show the correction made to the ephemeris of these satellites for better predicting the stellar occultations. In section 4, we present the predictions of the stellar occultations by irregular satellites and how they were made. Some tests made to confirm the pre-

dictions are presented in section 5 and the conclusions are given in section 6.

2. Scientific Rationale

As explicited in section 1, there is no consensus on a single model about the region where the irregular satellites were formed.

Phoebe, the most studied irregular satellite, was identified by Clark et al. (2005) that its surface is probably covered by material of cometary origin. It was also stated by Johnson & Lunine (2005) that if the porosity of Phoebe would be of about 15%, Phoebe would have an uncompressed density similar to those of Pluto and Triton.

Triton is a special satellite. Its orbit is retrograde and inclined, but quasi-circular and very close to the planet compared to the irregular ones. Because Triton's orbit is very small and its precession is not dominated by Solar perturbations, Triton is frequently excluded of the irregular satellites' class, but studied together by many authors (Sheppard 2005; Jewitt & Haghighipour 2007).

Similarly to the irregular satellites, Triton was probably capture in the early Solar System and may have a similar origin as the TNOs (Agnor & Hamilton 2006). Differently, Triton is bigger than the irregular satellites by an order of magnitude and has an atmosphere. The main objective to study Triton by stellar occultation is to understand the evolution of its atmosphere due to Triton's complicated and extreme seasonal cycle (McKinnon & Kirk 2007).

3. Correction of the ephemeris

Gomes-Júnior et al. (2015) published 6523 precise positions for 18 irregular satellites from observations made at the Observatório do Pico dos Dias (OPD), Observatoire Haute-Provence (OHP) and European Southern Observatory (ESO) between 1992 and 2014. They showed that the orbits of the irregular satellites of the giant planets have systematic errors. The offsets of the observations relative to the JPL ephemeris could be up to 200 mas for some satellites. These differences could be associated with errors in their orbital elements.

Making a new model for the orbits of these objects would demand a lot of time and delay the publication of predictions of possible events to occur in the very near future. Thus, we utilized the ephemeris offsets obtained by Gomes-Júnior et al. (2015) to identify error patterns in the ephemeris. The error patterns in right ascension and in declination could be used to extrapolate the offsets to the satellite ephemeris by the time of the predicted occultation, improving it. Plots of the offsets over time and true anomaly (see Fig. 3 and 3 for Carme) clearly show the systematic errors in the JPL ephemeris.

The two kinds of error or offset patterns adopted depending on the case are given by Eqs. 1 and 2:

$$F(t, f) = p[0] \times t + p[1] \times \sin(f) + p[2] \times \cos(f) + p[3], \quad (1)$$

$$F(t, f) = p[0] \times \sin\left(\frac{2\pi}{p[1]} \times t + p[2]\right) + p[3] \times \sin(f) + p[4] \times \cos(f) + p[5], \quad (2)$$

where $F(t, f)$ is the offset obtained, t is time in years counting from J2000.0 and f is the true anomaly. The patterns could be

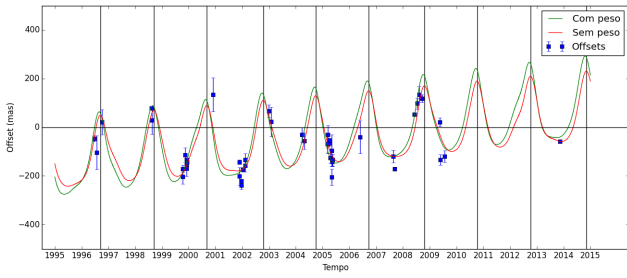


Fig. 1. Offsets of the declination of Carme by time. *Figura só para visualização, vou colocar alguma melhor depois*

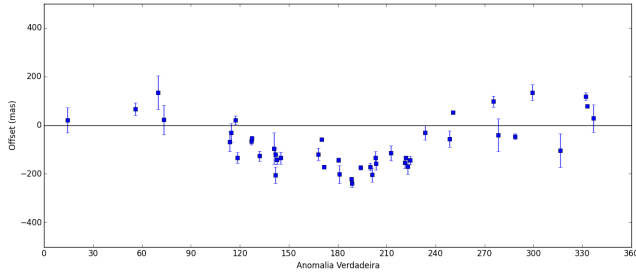


Fig. 2. Offsets of the declination of Carme by true anomaly. *Figura só para visualização, vou colocar alguma melhor depois*

applied for right ascension as well as for declination ephemeris offsets.

Falta justificar as funções

4. Prediction of occultations

The prediction of the occultations was made by crossing the stellar coordinates and proper motions of the UCAC4 catalogue (Zacharias et al. 2013) with the corrected JPL ephemeris as presented in section 3. The search for stellar candidates follows the same procedure as presented by Assafin et al. (2010, 2012) and Camargo et al. (2014).

We predicted occultation for the 7 major irregular satellites of Jupiter: Ananke, Carme, Elara, Himalia, Lysithea, Pasiphae, and Sinope; Phoebe of Saturn and Triton and Nereid of Neptune.

For Triton and Nereid, the candidates for stellar occultations in 2015 and 2016 was searched using the WFI catalogue in the same way as the predictions for Centaurs and TNOs occultations by Assafin et al. (2010, 2012) and Camargo et al. (2014). This catalogue contains the stars in the path of Neptune in the sky up to mid-2016. The catalogue was generated by observations made at the ESO 2p2 telescope (IAU code 809) using the Wide Field Imager (WFI) CCD mosaic detector. The filter used was the broad-band R filter ESO#844 with $\lambda_c = 651.725$ nm and $\Delta\lambda = 162.184$ nm.

A total of 588 events (*Não estou contando ainda os eventos para Tritão*) were identified between January 2015 and December 2017. Table 2 exemplifies the catalogue of occultations generated and their parameters, which are necessary to produce occultation maps (see Fig. 3 as an example). Since these objects are very small, the duration of each event is a few seconds.

The ESA astrometry satellite GAIA (de Bruijne 2012) catalogue is expected to be released in the end of 2016. The precise star positions to be derived by GAIA will render better predictions with the only source of error being the ephemeris. The work of Gomes-Júnior et al. (2015) will be revised with the GAIA catalogue and the predictions from 2017 onwards will be better pre-

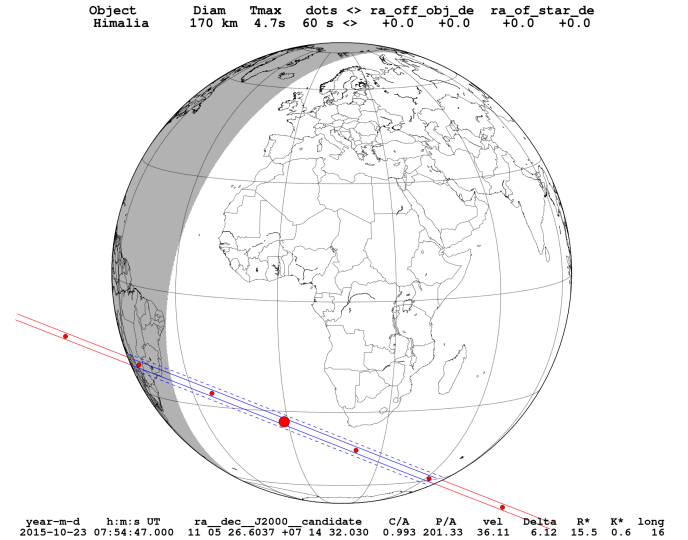


Fig. 3. Occultation map for Himalia regarding to the second event sampled in Table 2

dicted. For a matter of precaution and preparations of campaigns, we publish stellar occultations with UCAC4 until 2017.

5. Occultation tests

Observe a stellar occultation by an irregular satellites demands a great effort. The shadow covers a very restricted area on Earth because the irregular satellites are small. So, before we start a large observational campaign, we tested some occultation predictions for larger objects, to assess the quality of the prediction.

The tests consisted in observing the object and star to be occulted near the event when the two objects were present in the same field of view (FOV), preferably when the objects were close to each other. Thus, the relative positions between the two objects had minimal influence of the errors of the reference catalogue of stars used and possible field distortions (Peng et al. 2008, and references therein). The offsets of the positions of the star and of the satellites were used to check the original predictions.

Two occultation tests were performed, one by Himalia that occurred on March 3, 2015 and the second by Elara that occurred on March 30, 2015. For each event, four situations were considered: the first with the nominal positions of the star and the satellite to the predicted time; the second with the offset calculated as described in section 3; the third with star and satellite offsets from observations made a few days before the occultation when the two objects were separated (different FOV); and the fourth from observations made when the star and the satellite were close in the same FOV.

Figure 4 shows four zoomed in occultation maps corresponding to each of the four situations for Himalia. The map 4a is the nominal prediction with the coordinate of the star given by the catalogue and that of the satellite from the ephemeris. We then corrected the positions of the satellite by an offset calculated by the method showed in section 3 to make the map 4b. The map 4c was made from obtained positions on February 22 observed with the Zeiss telescope (Diameter = 0.6m; FOV = 12'6; pixel scale = 0'37/px) at the Observatório do Pico dos Dias (OPD, IAU code 874, 45°34'57"W, 22°32'04"S, 1864m). On that day, Himalia and the star were observed in separate FOVs as they were still

Table 2. Stellar occultation sampled predictions for Himalia **Consertar tabela**

d m Year	h m s	RA (ICRS) Dec	C/A	P/A	v	D	R*	λ	LST	Δe_{α^*}	Δe_{δ}	pm
07 10 2015	21 52 34.	10 53 40.1835 +08 21 00.489	0.465	200.31	39.31	6.25	16.6	179.	09:48	-31.0	-13.0	ok
23 10 2015	07 54 50.	11 05 26.6037 +07 14 32.030	1.017	201.33	36.11	6.12	15.5	16.	08:59	-31.0	-13.0	ok
31 10 2015	00 24 19.	11 10 56.2964 +06 42 07.110	1.801	21.84	33.94	6.04	16.9	123.	08:34	-31.0	-13.0	ok
07 11 2015	21 22 53.	11 16 14.3041 +06 10 05.194	0.306	202.36	31.33	5.94	16.2	162.	08:09	-31.0	-13.0	ok
08 11 2015	04 27 21.	11 16 25.7881 +06 08 55.566	1.077	202.38	31.23	5.94	16.9	55.	08:08	-31.0	-13.0	ok

Notes. Entries included: day of the year and UTC time of the prediction; right ascension and declination of the occulted star - in the original table, these coordinates are immediately followed by the geocentric astrometric equatorial coordinates of the satellite (corrected the computed ephemeris offset using Eqs 1 or 2); C/A: the geocentric closest approach, in arcseconds; P/A: the planet position angle with respect to the occulted star at C/A, in degrees; velocity in plane of sky, in km s^{-1} : positive = prograde, negative = retrograde; D: planet range to Earth, in AU; R*: normalized magnitude to a common shadow velocity of 20 km s^{-1} by the relationship $\text{Mag}^* = \text{Mag}_{\text{actual}} + 2.5 \times \log 10 \left(\frac{\text{velocity}}{20 \text{ km s}^{-1}} \right)$. A value of 50.0 means that the star is not in the 2MASS; λ : east longitude of subplanet point in degrees, positive towards east; LST: UT + λ : local solar time at subplanet point, hh:mm; Δe_{α^*} and Δe_{δ} : computed offsets in mas applied to the ephemeris right ascension and declination, respectively; pm: ok = proper motion applied, no = no proper motion applied; catalogue cross-identification (ct) = uc (UCAC2), 2m (2MASS), fs (field star); E_{α^*} and E_{δ} : uncertainties (mas) in right ascension and declination. A value of 9999 means that there was no estimation of the respective uncertainty; μ_{α^*} and μ_{δ} : proper motions in right ascension and declination, respectively (mas/year).

Table 3. Comparison between the predictions of the Himalia occultation at March 03, 2015. **Ainda vou terminar de preencher a tabela e tem que ver direito o offset do ajuste**

Difference from nominal prediction		
Method	Instant of C/A	C/A
Nominal	00:39:25 UTC	0°7'14
Offset		
Feb. 22 Obs.	+12s	-33mas (109km)
Mar. 03 Obs.	-10s	-19mas (61km)

far apart. On the night of the event, March 3, the objects were observed with Perkin-Elmer telescope (Diameter = 1.6m; FOV = 5'8; pixel scale = 0'17/px) at OPD just over an hour after the time scheduled for the event. Satellite and star were separated by about 16 arcsec, so very close to each other. From the calculated offsets, the map 4d was generated. Notice that the shadow path was not predicted to cross the OPD. This was not necessary for testing the prediction.

In this event, it is possible to see that the shade does not vary by much among the four maps suggesting that there was a good probability of observing the event. In fact, the biggest differences between the shadows of the four maps were **22s and 109km** in the direction perpendicular to the shadows (see table 3).

The second test was with the satellite Elara, which is the second largest irregular satellite of Jupiter. The event was predicted to occur at March 30, 2015. The observations were made on March 25 and April 2, 2015 with the Zeiss telescope. On the night of April 2 they could still be observed in the same FOV. Due to Elara being fainter than Himalia by 2 magnitudes, dispersions of the satellite positions on both nights ended up being higher than for Himalia. Still, the differences between the maps obtained were relatively small. The biggest differences between them were 74s along the shadow path and 307km perpendicular to it (see table 4).

6. Discussion

We presented stellar occultations for the period of 2015-2017 for seven irregular satellites of Jupiter: Ananke, Carme, Elara, Himalia, Lysithea, Pasiphae, and Sinope; one satellite of Saturn: Phoebe; and two satellites of Neptune: Triton and Nereid. The

Table 4. Comparison between the predictions of Elara occultation at March 30, 2015. **Ainda vou terminar de preencher a tabela e tem que ver direito o offset do ajuste**

Difference from nominal prediction		
Method	Instant of C/A	C/A
Nominal	01:45:15 UTC	1°1'39
Offset		
Mar. 25 Obs.	-59 s	-17mas (61km)
Apr. 02 Obs.	+15 s	-89mas (307km)

Table 5. Number of stellar occultations for each satellite from 2015 up to 2017

Satellite	2015	2016	2017	Total
Ananke				
Carme				
Elara				
Himalia				
Lysithea				
Pasiphae				
Sinope				
Phoebe	13	22	98	133
Nereid	40	11	1	52
Triton				

procedure used was the same that predicted stellar occultations by Pluto and its satellites in Assafin et al. (2010) and by Centaurs and TNOs in Assafin et al. (2012) and Camargo et al. (2014).

The candidate stars was searched in the UCAC4 catalogue, except for the candidates in 2015 and 2016 for Triton and Nereid. In this case, we used the WFI catalogue that was generated from observations made with ESO2p2/WFI CCD mosaic that covered the path of Neptune in the sky-plane up to 2016.

In table 5 it's presented the number of stellar occultations predicted by year for each satellite.

Acknowledgements. ARG-J thanks the financial support of CAPES. MA thanks the CNPq (Grants 473002/2013-2 and 308721/2011-0) and FAPERJ (Grant E-26/111.488/2013). RV-M thanks grants: CNPq-306885/2013, Capes/Cofecub-2506/2015, Faperj/PAPDRJ-45/2013. JIBC acknowledges CNPq for a PQ2 fellowship (process number 308489/2013-6). FB-R acknowledges PAPDRJ-FAPERJ/CAPES E-43/2013 number 144997, E-26/101.375/2014. BEM thanks the financial support of CAPES.

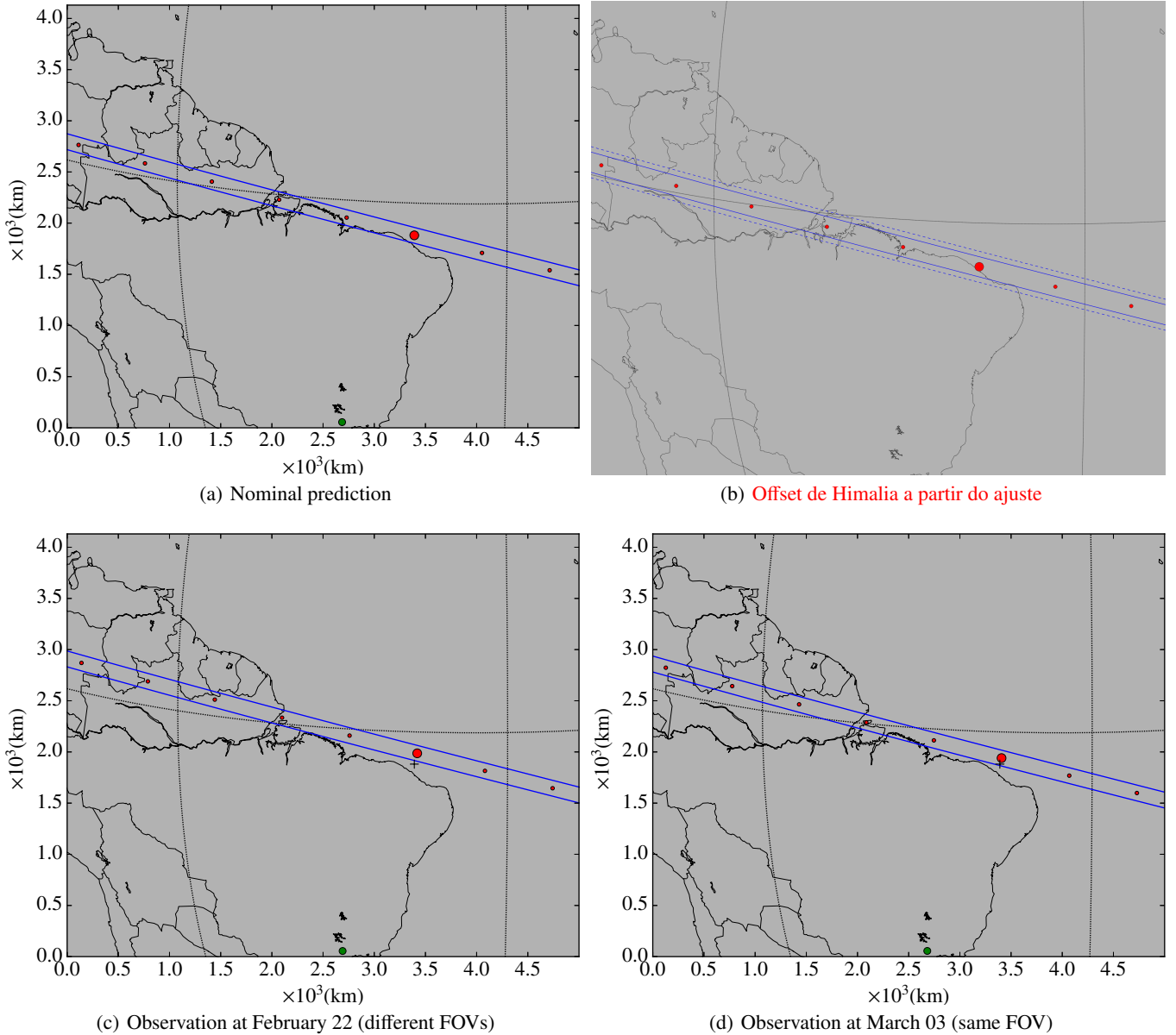


Fig. 4. Predictions for Himalia: The big red dot show the geocentric closest approach of the shadow. The black "+" marks at maps (b,c,d) are the nominal prediction closest approach for reference. The small red ones are the center of the shadow separated by one minute. The straight lines show the size of the shadow. 4a is the map using the nominal positions of the star and satellite. 4b shows the shadow given an estimated offset for the position of Himalia related to the JPL ephemeris obtained in section 3. In 4c we apply offsets to the positions of star and satellite accordingly the observations made at February 22. 4d is as in 4c but with observations made at March 03 when the objects were close to each other. The green dot at the bottom of the maps is the location of Observatório do Pico dos Dias. **Figura b será mudada após confirmarmos o offset para Himalia**

References

- Agnor, C. B. & Hamilton, D. P. 2006, *Nature*, 441, 192–194
- Assafin, M., Camargo, J. I. B., Vieira Martins, R., et al. 2010, *Astronomy & Astrophysics*, 515, A32
- Assafin, M., Camargo, J. I. B., Vieira Martins, R., et al. 2012, *Astronomy & Astrophysics*, 541, A142
- Braga-Ribas, F., Sicardy, B., Ortiz, J. L., et al. 2014, *Nature*, 508, 72–75
- Camargo, J. I. B., Vieira-Martins, R., Assafin, M., et al. 2013, *Astronomy & Astrophysics*, 561, A37
- Camargo, J. I. B., Vieira-Martins, R., Assafin, M., et al. 2014, *Astronomy & Astrophysics*, 561, A37
- Clark, R. N., Brown, R. H., Jaumann, R., et al. 2005, *Nature*, 435, 66–69
- de Bruijne, J. H. J. 2012, *Astrophysics and Space Science*, 341, 31–41
- Gomes, R., Levison, H. F., Tsiganis, K., & Morbidelli, A. 2005, *Nature*, 435, 466–469
- Gomes-Júnior, A. R., Assafin, M., Vieira-Martins, R., et al. 2015, *Astronomy & Astrophysics*
- Grav, T. & Bauer, J. 2007, *Icarus*, 191, 267–285
- Grav, T., Holman, M. J., Gladman, B. J., & Aksnes, K. 2003, *Icarus*, 166, 33–45
- Jacobson, R., Brozović, M., Gladman, B., et al. 2012, *The Astronomical Journal*, 144, 132
- Jewitt, D. & Haghighipour, N. 2007, *Annual Review of Astronomy and Astrophysics*, 45, 261–295
- Johnson, T. V. & Lunine, J. I. 2005, *Nature*, 435, 69–71
- McKinnon, W. & Kirk, R. 2007, *Encyclopedia of the Solar System*, 483–502
- Morbidelli, A., Levison, H. F., Tsiganis, K., & Gomes, R. 2005, *Nature*, 435, 462–465
- Nesvorný, D., Alvarellos, J. L. A., Dones, L., & Levison, H. F. 2003, *AJ*, 126, 398–429
- Nesvorný, D., Beaugé, C., & Dones, L. 2004, *AJ*, 127, 1768–1783
- Nesvorný, D., Vokrouhlický, D., & Deienno, R. 2014, *ApJ*, 784, 22
- Nesvorný, D., Vokrouhlický, D., & Morbidelli, A. 2007, *AJ*, 133, 1962–1976
- Ortiz, J. L., Sicardy, B., Braga-Ribas, F., et al. 2012, *Nature*, 491, 566–569
- Peng, Q., Vienne, A., Lainey, V., & Noyelles, B. 2008, *Planetary and Space Science*, 56, 1807–1811

- Porco, C. C., West, R. A., McEwen, A., et al. 2003, *Science*, 299, 1541–1547
- Rettig, T., Walsh, K., & Consolmagno, G. 2001, *Icarus*, 154, 313–320
- Sheppard, S. S. 2005in (Cambridge University Press (CUP)), 319
- Sicardy, B., Ortiz, J. L., Assafin, M., et al. 2011, *Nature*, 478, 493–496
- Thomas, P. 2000, *Icarus*, 148, 587–588
- Thomas, P. 2010, *Icarus*, 208, 395–401
- Thomas, P., Veverka, J., & Helfenstein, P. 1991, *J. Geophys. Res.*, 96, 19253
- Tsiganis, K., Gomes, R., Morbidelli, A., & Levison, H. F. 2005, *Nature*, 435, 459–461
- Zacharias, N., Finch, C. T., Girard, T. M., et al. 2013, *The Astronomical Journal*, 145, 44